Applying the exponential convergence method: Shell-model binding energies of $0f_{7/2}$ nuclei relative to ^{40}Ca

Mihai Horoi,[1] B. Alex Brown,[2,3] and Vladimir Zelevinsky[2,3]
[1]*Physics Department, Central Michigan University, Mount Pleasant, Michigan 48859*
[2]*National Superconducting Cyclotron Laboratory, East Lansing, Michigan 48824*
[3]*Department of Physics and Astronomy, Michigan State University, East Lansing, Michigan 48824*
(Received 18 June 2001; published 15 January 2002)

It was suggested earlier that, due to the statistical properties of complicated many-body dynamics, the energies of low-lying nuclear states in large shell model spaces converge to their exact values exponentially as a function of the dimension in progressive truncation. Applying the exponential convergence algorithm as a practical method of extrapolation we calculated ground-state energies, spins, and isospins of the lowest $|\Delta(N-Z)|$ nuclides from ^{42}Ca to ^{56}Ni using the fp-shell model and the FPD6 interaction. The binding energies relative to ^{40}Ca are compared with the experimental values. The deviation can be accounted by adding monopole terms to the single-particle energies and two-body matrix elements.

DOI: 10.1103/PhysRevC.65.027303 PACS number(s): 21.60.Cs, 21.10.Dr, 21.60.Ka, 27.40.+z

Shell-model calculations of the ground state and low-lying excited states are essential for our understanding of nuclear dynamics and the (effective) nuclear forces. The nuclear shell model with the effective two-body interactions in a restricted Hilbert space is the best available theoretical tool for calculating the properties of the low-lying states. The region of the nuclear chart between Ca and Ni is especially important for coming radioactive beam experiments and astrophysical applications.

However, full shell-model calculations are being limited by the exponential increase of the dimension of the many-body Hilbert space with the number of valence nucleons. For example, the *m*-scheme dimension for 20 nucleons in the fp shell is 2,292,604,744. Full sd-shell model calculations were possible 20 years ago [1], but a similar shell-model calculation for all nuclei in the fp shell is not yet available. In the past decade, several approximate methods were proposed to deal with the dimensionality problem. Among them are the shell-model Monte Carlo (SMMC) [2], quantum Monte Carlo diagonalization (QMCD) [3], and exponential convergence method (ECM) [4].

In the ECM, possible configurations of valence nucleons in the finite number of single-particle states are ordered according to their centroid energies found with the aid of the methods of statistical spectroscopy [6,7]. In a truncation scheme [5] for the low-lying states, higher configurations can be consecutively added to the many-body model space in order of their centroid values. It was shown in Ref. [4] that, as a function of the dimension of truncated Hilbert space, the energies of the low-lying states converge exponentially to their exact values. The physics underlying this numerical observation is associated [4,8] with the exponentially decreasing admixtures of energetically distant configurations both in the realistic shell model and in random matrices. Being analogous to the exponential localization of coordinate wave functions of electronic states in disordered solids [9], the same physics is revealed in the exponential behavior of the remote energy tails of the strength functions of simple states in complex atoms [10] and nuclei [11]. The strict mathematical arguments were developed for tridiagonal matrices [4]. This property of exponential convergence can be successfully used to predict the exact energy of the many-body eigenstates. According to Ref. [5], the initial truncation size should exceed a certain value related to the spreading width of typical basis states found from the Hamiltonian matrix prior to its diagonalization. It was also suggested that the matrix elements of observables can be extracted by a similar procedure.

In this Brief Report we develop the ECM into a practical tool and calculate energies, spins, and isospins of the ground states for the nuclei from ^{42}Sc to ^{56}Ni. We performed the calculation for the nuclides having the lowest isospin projection (0 for even A, and 1/2 for odd A) because they include the largest amount of correlations for a given number of valence nucleons. We use the FPD6 interaction [12] which was designed to describe accurately nuclei with $A=44-46$, and it is known to better describe the energy gaps around ^{56}Ni [13]. The results for the calculated ground-state energies and quantum numbers $J^{\pi}T$ are summarized in Table I. In all cases but one, the experimental spin J is correctly reproduced. The only exception is for $A=45$, where the three lowest states with spins $J=3/2,5/2$, and 7/2 are nearly degenerate within 100 keV both in theory and experiment. Parities and isospins (when available) are always reproduced correctly. The *m*-scheme dimensions are listed in Table II along with the dimensions of the JT space corresponding to the ground-state quantum numbers. Energies of the nuclei up to $A=49$ (less than ten valence nucleons) were calculated using full shell-model spaces; for $A>49$ the ECM was used. The ground-state energy for ^{56}Ni, -203.280 MeV, is about 200 keV lower than the recently reported QMCD value [13]. A similar study using the code NATHAN [14] and the KB3 interaction was recently reported but $A=53$ and 55 nuclei were not calculated.

To demonstrate the ECM at work we include here two typical cases: the ground state of ^{48}Cr, Fig. 1 (an application to the excited 2^+ state of ^{48}Cr was shown in Ref. [4]), and ^{49}Cr, Fig. 2. Both figures show the dynamics of the corre-

TABLE I. Theoretical and experimental ground state energies (in MeV), spins, and isospins.

A	Nuclei	$E_{\text{g.s.}}$ (SM)	$E_{\text{g.s.}}$ (exp)	$J^\pi T$	$(J^\pi T)_{\text{exp}}$
42	^{42}Sc	−19.814	−20.026	0^+1	0^+1
43	^{43}Sc	−32.104	−32.115	$7/2^-1/2$	$7/2^-1/2$
44	^{44}Ti	−48.142	−48.381	0^+0	0^+0
45	^{45}Ti	−57.782	−57.453	$3/2^-1/2$	$7/2^-1/2$
46	^{46}V	−70.696	−71.009	0^+1	0^+1
47	^{47}V	−83.936	−83.864	$3/2^-1/2$	$3/2^-1/2$
48	^{48}Cr	−99.970	−100.030	0^+0	0^+0
49	^{49}Cr	−110.029	−110.416	$5/2^-1/2$	$5/2^-1/2$
50	^{50}Mn	−122.400	−123.292	0^+1	0^+1
51	^{51}Mn	−135.340	−136.734	$5/2^-1/2$	$5/2^-1/2$
52	^{52}Fe	−150.980	−152.631	0^+0	0^+0
53	^{53}Fe	−160.880	−163.020	$7/2^-1/2$	$7/2^-1/2$
54	^{54}Co	−173.800	−176.114	0^+1	0^+1
55	^{55}Co	−187.000	−189.861	$7/2^-1/2$	$7/2^-1/2$
56	^{56}Ni	−203.280	−205.992	0^+0	0^+0

sponding energy eigenvalue as a function of the truncated dimension of the JT-projected shell-model basis. Each consecutive truncation step includes new shell-model partitions (with increasing energy centroids) in their entirety. The full fp-shell dimensions for these two cases are 9741 and 232514, respectively. One can see from Fig. 2 using the logarithmic energy scale that for small dimensions the decrease of the truncated ground-state energy is faster than exponential (low dimension data for ^{48}Cr are not included in Fig. 1 but they behave similarly to the ^{49}Cr case). This different behavior can be attributed to a relatively coherent contribution of the lowest centroid configurations to the structure of the ground state as compared to more chaotic contributions of the high centroid configurations.

TABLE II. Dimensions of the JT-projected basis corresponding to the ground-state quantum numbers (see Table I), and maximum m-scheme dimensions.

A	Nuclei	JT dim	m-scheme dim.	$(E_s-E_m)/\sigma$
42	^{42}Sc	4	60	
43	^{43}Sc	61	472	
44	^{44}Tm	66	4000	
45	^{45}Tm	1250	21691	
46	^{46}V	1514	121440	3.0
47	^{47}V	18392	483887	2.9
48	^{48}Cr	9741	1963461	3.1
49	^{49}Cr	232514	6004205	3.3
50	^{50}Mn	134361	18600516	3.2
51	^{51}Mn	1417374	44993824	3.2
52	^{52}Fe	671159	109954620	3.2
53	^{53}Fe	7008147	214688113	3.5
54	^{54}Co	2299178	422818560	3.9
55	^{55}Co	19950699	675477701	4.0
56	^{56}Ni	2581576	1087455228	4.0

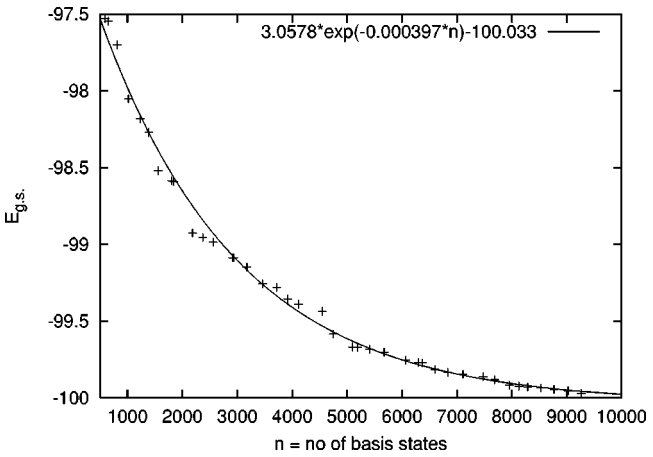

FIG. 1. Ground-state energy (in MeV) of ^{48}Cr versus the dimension of the truncated space.

It is important to have a working recipe for approximating the dimension where the exponential behavior starts. The 3σ truncation method was proposed in Ref. [5]. The coupling of various configurations can be quantified [7,15] with the help of the average width σ associated with each configuration [5,6] $\sigma^2=\langle H^2_{\text{off-diag}}\rangle_{\text{av}}$. Because of chaotic mixing at high level density, the widths σ are nearly the same for different partitions. In the strong coupling regime, the spreading widths of simple configurations [11] are close to $\Gamma\approx 2\sigma$. Therefore one can expect that the exponential regime starts beyond the energy distance of the order of 3σ [5]. In the last column of Table II we include the ratio $(E_s-E_m)/\sigma$, where E_s is the centroid energy of the configuration at which the exponential behavior starts, E_m is the lowest centroid energy, and σ is the width of the lowest configuration. As seen from this table, we indeed observe the exponential behavior starting at a configuration whose centroid energy is 3–4 σ above that for the lowest energy configuration.

The exponential convergence algorithm for finding ground-state energy works as follows.

(i) A set of configurations (partitions for a given particle number in a certain orbital space) to be included in the cal-

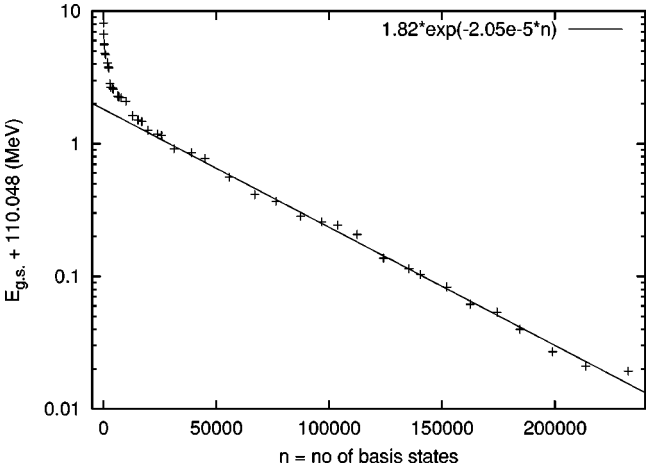

FIG. 2. Ground-state energy of ^{49}Cr versus the dimension of the truncated space.

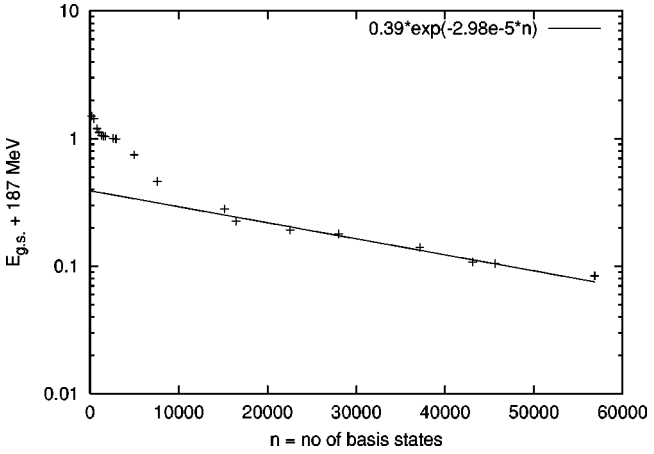

FIG. 3. Ground-state energy of ^{55}Co versus the dimension of the truncated space.

culation is generated. The number of configurations in a given model space is much lower than the shell-model dimension. For example, the highest *m*-scheme dimension for $A=49$ in the fp-shell is 6,004,205, while the number of configurations is 184.

(ii) The average centroids (Hamiltonian traces) for these configurations are calculated using the prescription of statistical spectroscopy [6,7].

(iii) The configurations are ordered according to their average centroids. This order is different from the usual particle-holes (p-h) scheme. For example, in the fp shell some $8p$-$8h$ configurations come lower than many of $4p$-$4h$ configurations, where the particle (p) and hole (h) refer to excitations from the $0f_{7/2}$ orbital to one of the $0f_{5/2}$, $1p_{3/2}$, or $1p_{1/2}$ orbitals.

(iv) Shell-model matrices are built for the truncated spaces consecutively including into calculations the configurations in their ''natural'' order established in (iii).

(v) The energies of the low-lying (ground in this article) states are calculated using a Lanczos eigenvalue solver. The step (v) is repeated 5–10 times by expanding the space with inclusion of new partitions.

(vi) The graph of energy vs JT dimension is plotted (e.g., Fig. 3), the beginning of the exponential tail is identified, and a fit with the expression

$$E(n)=C+Be^{-\gamma n} \tag{1}$$

is performed. To predict ground-state energy one should evaluate $E(N)$, where N is the full JT dimension of the original model space. Most of the time the parameter C in Eq. (1) is a good approximation for $E(N)$. Examples of parametrization (1) are included in Figs. 1–3.

It is difficult to assign errors to the predicted energy values because of the fluctuations around the pure exponential behavior. However, one can associate the errors in the parameter C obtained from the fitting algorithm (see, e.g., Ref. [16]) with the error in the predicted energy. For the cases presented in Table I the errors range from 20 to 200 keV. These errors are significantly lower than the ones obtained with other methods, such as SMMC [17].

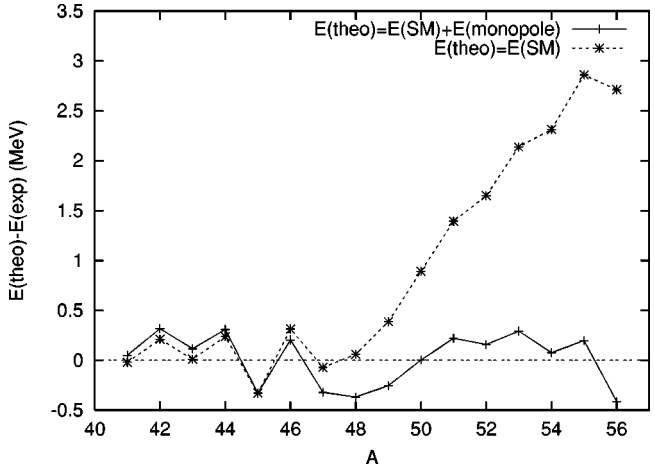

FIG. 4. Difference between the theoretical ground-state energies calculated with the FPD6 interaction plus the monopole correction, Eq. (4), and experimental values corrected for Coulomb effects.

In order to compare the ground-states energies in Table I with experiment, one must correct the experimental values relative to the core of ^{40}Ca for Coulomb effects [17,14]

$$H_C=\epsilon_\pi N_\pi+V_{\pi\pi}\frac{N_\pi(N_\pi-1)}{2}+V_{\pi\nu}N_\pi N_\nu. \tag{2}$$

Here $N_\pi(N_\nu)$ denotes a number of valence protons (neutrons), and the following values of the parameters were used [14]: $\epsilon_\pi=7.440$ MeV, $V_{\pi\pi}=0.274$ MeV, $V_{\pi\nu}=-0.049$ MeV. They were obtained [14] by fitting the Coulomb displacement energies for analog nuclei between $A=42$ and $A=64$.

Table I presents theoretical and experimental ground-state energies of all considered nuclei relative to the core of ^{40}Ca. The general agreement seems to be good, however, toward $A=56$ the binding energy predicted by the FPD6 interaction is slightly smaller than the experimental value. In Fig. 4 we plot (stars) the difference between theoretical ground-state energies calculated with the FPD6 interaction and corresponding experimental energies corrected for Coulomb effects. The results show a generally good agreement with experiment for nuclei with $A=42$ to 48, but the discrepancy increases up to 3 MeV around $A=56$.

Following Ref. [14], the simplest correction we can make is to add monopole terms to the single-particle energies and matrix elements of the FPD6 interaction in a form that does not change the wave function:

$$E(\text{theo})=E(\text{SM})+E_{\text{monopole}}, \tag{3}$$

where

$$E_{\text{monopole}}=en+\frac{1}{2}n(n-1)v\left(\frac{42}{n+42}\right)^{0.35}. \tag{4}$$

Here $n=A-40$ is the number of valence nucleons in the fp shell, e is the one-body monopole contribution to average single-particle energy of the major shell, v is the average

monopole contribution to the two-body matrix elements. The mass dependence in the equation is the same as that assumed for the FPD6 interaction.

The parameters e and v were determined by fitting the data in Table I and ^{41}Ca (whose energy relative to the core of ^{40}Ca is the $0f_{7/2}$ single-particle energy in the FPD6 interaction). Using Eq. (3) we obtain $e=0.0707$ MeV and $v=-0.0355$ MeV, The energy differences with the monopole contribution included are shown by crosses in Fig. 4. The overall quality of the resulting fit is very good; the mean square deviation is 0.272 MeV.

In conclusion, we have calculated the ground-state energies, spins and isospins for the nuclides from ^{42}Sc to ^{56}Ni using the exponential convergence method [4] and the FPD6 interaction. The calculated spins and isospins reproduce well the experimental results. The ground-state energies are also in good agreement with data after the single-particle energies are slightly shifted, and a small monopole correction is added to the two-body matrix elements of the FPD6 interaction. Full fp calculations of the ground state energies of $A=53$ and $A=55$ nuclei are reported, to our knowledge, for the first time. The results indicate that the ECM is a powerful tool for calculating the properties of low-lying states when the full large-scale shell-model diagonalization is not feasible. The FPD6 interaction with monopole corrections can be successfully used to describe the ground-state properties of the fp nuclei. Additional studies along the same line for the excited states, transition probabilities and other observables are necessary.

The authors acknowledge support from U.S. NSF Grant Nos. PHY-0070911 and DMR-9977582.

[1] B.A. Brown and B.H. Wildenthal, Annu. Rev. Nucl. Part. Sci. **38**, 29 (1988).
[2] D.J. Dean, P.B. Radha, K. Langanke, Y. Alhassid, S.E. Koonin, and W.E. Ormand, Phys. Rev. Lett. **72**, 4066 (1994); Y. Alhassid, D.J. Dean, S.E. Koonin, G. Lang, and W.E. Ormand, *ibid.* **72**, 613 (1994).
[3] M. Honma, T. Mizusaki, and T. Otsuka, Phys. Rev. Lett. **75**, 1284 (1995); **77**, 3315 (1996).
[4] M. Horoi, A. Volya, and V. Zelevinsky, Phys. Rev. Lett. **82**, 2064 (1999).
[5] M. Horoi, B.A. Brown, and V. Zelevinsky, Phys. Rev. C **50**, R2274 (1994).
[6] J.B. French and K.F. Ratcliff, Phys. Rev. C **3**, 94 (1971).
[7] S.S.M. Wong, *Nuclear Statistical Spectroscopy* (Oxford University Press, New York, 1986).
[8] V. Zelevinsky, in *Highlights of Modern Nuclear Structure*, edited by A. Covello (World Scientific, Singapore, 1999), p. 223.
[9] J. Rammer, *Quantum Transport Theory* (Perseus, Reading, MA, 1998).
[10] V.V. Flambaum, A.A. Gribakina, G.F. Gribakin, and M.G. Kozlov, Phys. Rev. A **50**, 267 (1994).
[11] N. Frazier, B.A. Brown, and V. Zelevinsky, Phys. Rev. C **54**, 1665 (1996).
[12] W.A. Richter, M.G. van der Merwe, R.E. Julies, and B.A. Brown, Nucl. Phys. **A523**, 325 (1991).
[13] T. Otsuka, M. Honma, and T. Mizusaki, Phys. Rev. Lett. **81**, 1588 (1998).
[14] E. Caurier *et al.*, Phys. Rev. C **59**, 2033 (1999).
[15] V. Zelevinsky, B.A. Brown, N. Frazier, and M. Horoi, Phys. Rep. **276**, 315 (1996).
[16] P. R. Bevigton, *Data Reduction and Error Analysis for Physical Science* (McGraw-Hill, New York, 1969).
[17] K. Langanke, D.J. Dean, P.B. Radha, Y. Alhassid, and S.E. Koonin, Phys. Rev. C **52**, 718 (1995).